



Modelling of Temperature Field in a Reactor Vessel Downcomer during Transients

Martin Prosimický¹⁾, Pavel Zácha¹⁾

¹⁾ Czech Technical University of Prague, Prague, Czech Republic

ABSTRACT

Detailed 3D modeling of fluid flow in currently operating and future reactors is an integral part of modern scientific research worldwide. The phenomenal increase of computational capabilities in the last decades made feasible not only a full 3D modeling of large systems but also an introduction of turbulence models and complex modeling details into the CFD codes, increasing the need for experimental data for code benchmarking. To reduce cost of obtaining experimental data in large facilities representing the integral reactor-vessel-loop system, international projects were established and the experimental database has been obtained. This paper presents validation of CFD code Fluent 6.0 against experimental data from such database.

KEY WORDS: CFD, fluid dynamics, Fluent, turbulent model, nuclear reactor.

INTRODUCTION

International Standard Problem No. 43 (ISP 43) [1] addresses the nuclear industries present capabilities of simulating fluid dynamics aspects of a subset of rapid boron dilution transients. Specifically, the exercise focuses on the sequence involving the transport of a boron-dilute slug following the actuation of a pump. The slug is formed on the primary side of the steam generator as a consequence of an interfacing system leak from the secondary unborated coolant.

Experimental data was collected using the University of Maryland 2x4 Thermal hydraulic Loop (UM 2x4 Loop) and the Boron-mixing Visualization Facility.

Four test series were run in the course of ISP Nr. 43 experimental program. The first and second (A and B series) are of major interest and are briefly described next. The first test is very simple and approaches a special effect type exercise; while the last one involves all integral test facility features of the UM 2x4 Loop. In test series A, the “clean” water is injected from an external tank, which effectively simulates the injection of a front rather than a slug. The test has the advantage of eliminating back-end distortions from data interpretation. All cold legs, except for the one used for front injection (CL A1), are isolated from the vessel. This limits the path of the fluid from the tank, through the cold leg and downcomer, up into the core and out through hot leg A (HL A). The front is injected using the CL A1 primary coolant pump. In test series B, the slug is injected into the bottom of steam generator A from an external tank. The primary system is then isolated, and the slug is set in motion by pump A1. The other cold legs remain isolated. The slug follows a closed path through CL A1, the downcomer, the lower plenum, the core, and returns to its initial position through HL A.

The B test series from the course of ISP Nr. 43 is analysed in this paper. The measured boundary conditions include the initial temperature of the primary system, the front/slug injection flowrate and temperature, and the pressure drop across the core. Temperature data is collected at 185 thermocouple positions in the downcomer and 38 positions in the lower plenum. The frequency of data acquisition for code predictions was set to 2 Hz, which corresponds to the acquisition frequency of the two experimental setups.

Program FLUENT

Calculations were performed using a Computational Fluid Dynamics (CFD) computer code FLUENT [2]. This program is based on Finite volume method, i.e., the fluid region is discretized into finite set of control volumes (tetrahedrons, pentahedrons and hexahedrons). The computational mesh is generated by the pre-processor - program GAMBIT.

FLUENT uses a control-volume-based technique to convert the governing equations to algebraic equations that can be solved numerically. This control volume technique consists of integrating the governing equations about each control volume, yielding discrete equations that conserve each quantity on a control-volume basis.

The connection between values at single cell and adjacent cells is done by interpolation scheme. FLUENT employs several turbulent models. These models have the following strengths and weaknesses:

- Spalart-Allmaras model
 - + Economical (1-equation.); good track record for mildly complex B.L. type of flows,
 - Not very widely tested yet; lack of submodels (e.g. combustion, buoyancy);

- STD $k - \epsilon$
 - + Robust, economical, reasonably accurate; large amount of accumulated performance data,
 - Mediocre results for complex flows involving severe pressure gradients, strong streamline curvature, swirl and rotation;
- RNG $k - \epsilon$
 - + Good for moderately complex behavior like jet impingement, separating flows, swirling flows, and secondary flows,
 - Subjected to limitations due to isotropic eddy viscosity assumption;
- Realizable $k - \epsilon$
 - + Offers largely the same benefits as RNG; resolves round-jet anomaly,
 - Subjected to limitations due to isotropic eddy viscosity assumption;
- Reynolds Stress Model
 - + Physically most complete model (history, transport, and anisotropy of turbulent stresses are all accounted for),
 - Consumes more CPU (2-3x than $k - \epsilon$ models); tightly coupled momentum and turbulence equations.

Program Gambit

The GAMBIT software package [2] is designed to help analysts and designers build and mesh models for CFD and other scientific applications. It has capability to produce structured and unstructured mesh for 2D and 3D problems solved by various finite volume method programs.

FLOW COMPUTATION

The main goal of this benchmarking calculation was to evaluate the capability of CFD codes, specifically FLUENT, to predict thermal field in a reactor vessel with complex inner structures and where 3-D mixing of flow streams of different temperatures in the downcomer and lower plenum play an important role. The temperature field is represented in the experiment by data obtained from thermocouples located at various positions in the vessel, especially in the downcomer. The simulation was performed in the time segment, where main changes in temperature occurred: between 9 (initiation of fluid flow) and 40 seconds.

FLUENT code provides a large variety of choices of physical models and discretization schemes, when setting up the problem. Some of these settings affect only numerical precision of the result and some affect the correctness of the results. The default settings, which guarantee convergence and stability of the computation, were employed (Table 2).

Coarse computational mesh can significantly reduce the accuracy of the results and to obtain good prediction sufficiently fine and high-quality mesh is necessary. To illustrate the affect of mesh quality on the results, sensitivity study to mesh quality was performed.

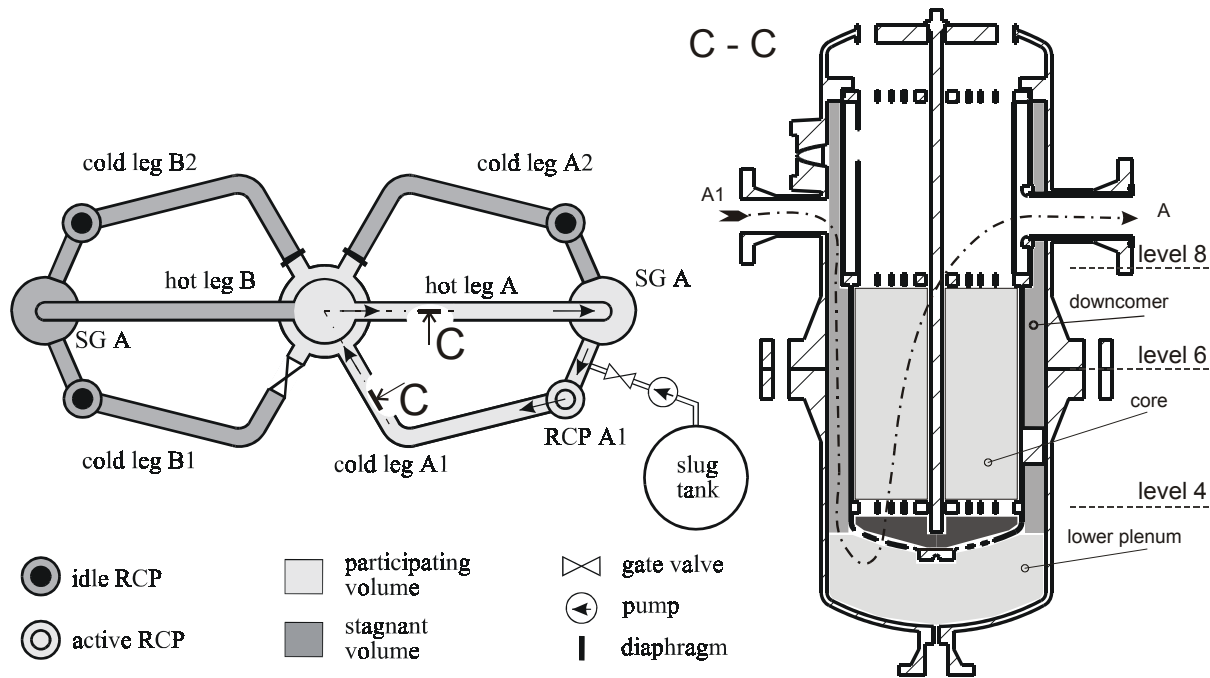


Figure 1 Top view of the facility and cross section through cold leg A1 and hot leg A.

Computational mesh

Computational mesh covers volumes from the inlet A1 to the outlet at one-half of the core (see Fig. 1).

Concerning mesh density of the most demanding location was the area around perforated elliptic bottom of the core barrel and of course the volume of the downcomer where the temperatures are calculated.

Three computational meshes were built. The mesh was unstructured, using tetrahedrons. These meshes differ in their density only at the zone of the downcomer. The total number of the cells for each mesh is given in Table 1:

I	352 338	II	496 451	III	1 300 000
---	---------	----	---------	-----	-----------

Table 1 Total number of cells for models with different mesh quality

FLUENT setup

The Standard $k-\epsilon$ turbulent model, which gives in most cases good results at relatively low computational effort, was used. The parameters used in the model are listed in Table 2:

Solver	Segregated
Formulation	Implicit
Inlet boundary conditions	Temperature and velocity perpendicular to inlet is set, as shown in Fig. 2 Turbulence intensity $I = 10\%$, hydraulic diameter $DH = 0,0762$ m
Outlet boundary condition	Outflow
Material	Water with density and viscosity specified by user-defined function, other properties were fixed
Initial temperature	342,35 K – taken as average temperature from all thermocouples in the vessel
Near wall condition	Standard wall function
Discretization	Pressure: standard; pressure-velocity coupling: SIMPLE; momentum, k , ϵ , energy: first order upwind
Unsteady formulation	1st-order implicit
Time step	0,2 s

Table 2 Boundary conditions and model parameters used in calculations

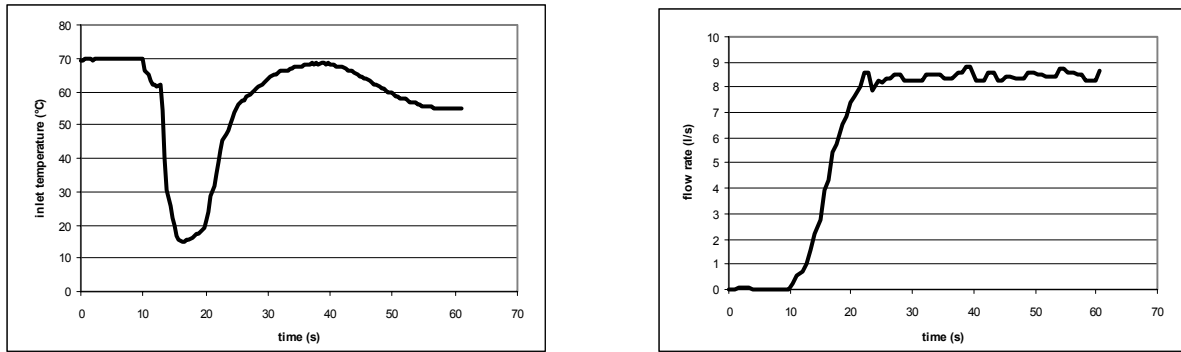


Figure 2 Boundary conditions at the inlet A1.



Figure 3 Streams in the downcomer at different times.

CALCULATED DEVELOPMENT OF DOWNCOMER FLOW

First it needs to be noted that the transient flow aspects strongly affect flow field in the downcomer and lower plenum in the beginning of the calculations. In the time span of 0 to 9 seconds, velocity in the entire reactor vessel is zero. In the beginning, the inlet velocity is small and the flow rate in the downcomer is along azimuthal coordinate distributed relatively uniformly. The differences in velocities are small and maximum and minimum velocities are on the azimuthal position of 0° and 180° , respectively.

As the time proceeds, the flow is gradually divided (approximately symmetrically) into two streams, which individually flow downwards through the downcomer into the lower plenum. This can be observed in Figure 3 (times 21.2s).

The rate at which the axis of these two streams approaches azimuthal position 180° depends on the inlet velocity of the entering flow. After some time the streams join at 180° and the resulting flow field at this position has the largest temperature non-uniformity in the downcomer. Temperature in these streams is closely associated with the inlet temperature. Even as the two streams are fully joined later, the interface between these streams is still visible on the temperature signature (if warmer coolant enters the reactor, lower temperature is observable in the middle of the stream, as indicated in Appendix 2, 36s, level 4 at 180°).

Flow in the downcomer can be with respect to the above discussion subdivided into 3 phases:

1. until the time of about 16 s: vertical velocity in the downcomer cross section sufficiently far from the inlet is nearly constant
2. between 16 s and about 25 s: two approximately same streams exist in the downcomer, one in each half of the downcomer
3. after 26 s: the two streams become one

COMPARISON OF EXPERIMENTAL AND COMPUTATIONAL DATA

Two types of graphs will be used to illustrate the distinction between the experiment and computation. Coolant temperatures at individual measurement levels in the downcomer in time are plotted in Fig. 4. Temperature angular distribution for selected levels and times is shown in Fig. 5, 6 and 7.

First group of graphs illustrate how the stream front moves from the inlet through the downcomer. Differences in average temperature between the experiment and the calculations can be explained with the help of the second group of graphs.

Characteristic difference between the experimental and calculated data can be observed for example on level 4 at time 24 s. This time is at the end of the second phase. The temperature of the entering flow at the inlet is still higher at this time by about 50 °C. The velocity at the inlet has been constant for about 3 s. The transit time for the fluid particle between the inlet to level 6 through one of the main stream is about 1.5 s. Prior to 1.5 s the temperature at inlet was 42 °C. The core of the stream does not preserve exactly the same temperature as the inlet temperature, but very close (little bit lower). This region can be clearly seen in Fig. 5. Between these streams is a domain, which was influenced to the least extent and preserved almost the original temperature of water. Temperature distribution in downcomer is very similar for the experiment and for the calculation. Differences between the maximum and minimum temperatures at individual levels are however, bigger for the calculation then for experiment.

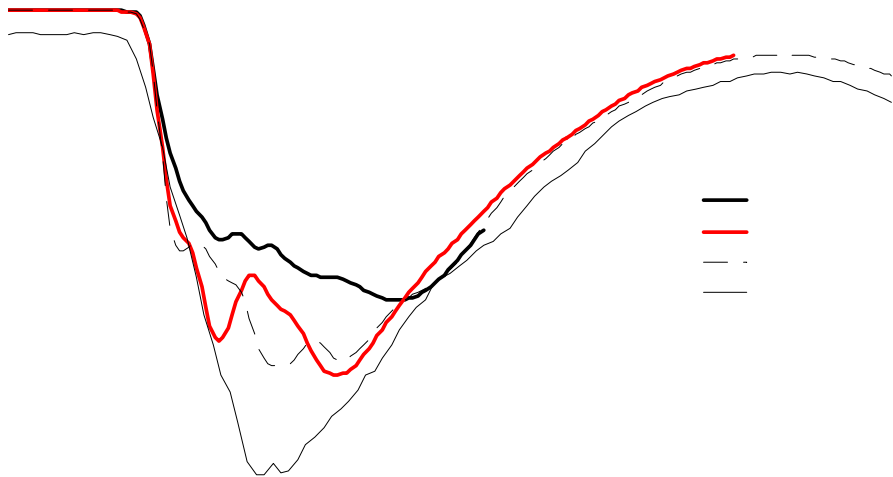
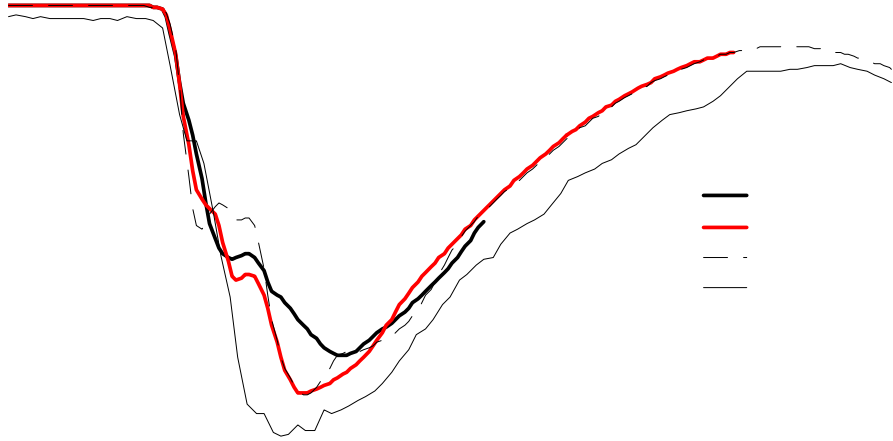
Calculations exhibit slower rate of temperature decrease along the mainstream and slower heat transport in the direction perpendicular to the main flow. This is most likely caused by viscosity model employed, because the $k-\epsilon$ turbulent models used in the calculations do not incorporate anisotropies in turbulent heat transport.

The calculated narrow, fast moving and cold streams, which flow through the downcomer in the second phase, affect the temperature in the downcomer to a less extent than the slow moving, but wider streams observed in the experiment. Thus, it follows that in the simulations, the cooler water will reach reactor core faster than in reality, where the water originally present in the downcomer is pushed out by a wide down coming stream.

Consequently, after the cold water from inlet reaches the downcomer, the average temperatures at all levels are higher than in reality. The effect of heat losses to surroundings can also contribute to this difference to some extent, but this is small second order effect. As the parameters at the inlet get more uniform with time, the differences between the predictions and experiment reduce.

REFERENCE

1. Gavrilas, M., Kiger K., OECD/CSNI ISP Nr. 43 Rapid Boron-dilution Transient Tests for Code Verification, University of Maryland USA, 2000.
2. www.fluent.com



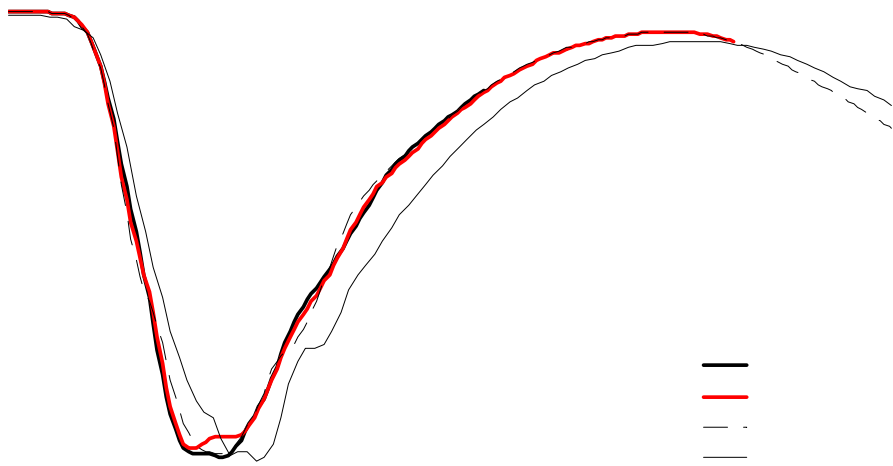
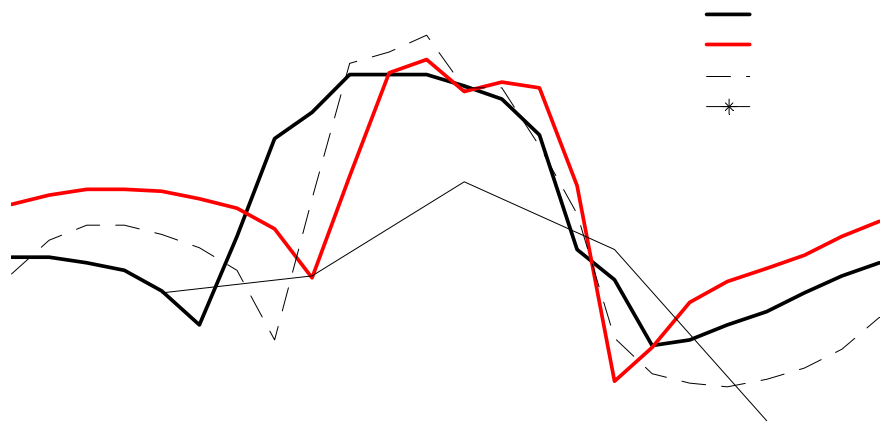
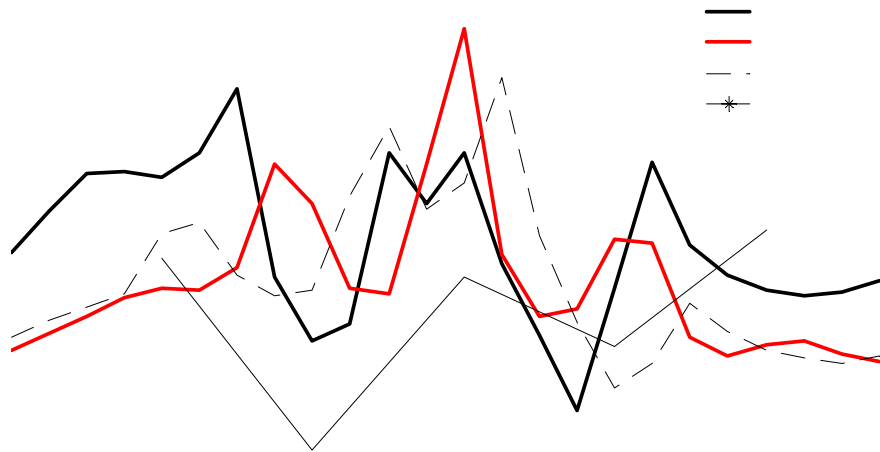


Figure 4 Average temperatures at levels 4, 6 and 8.



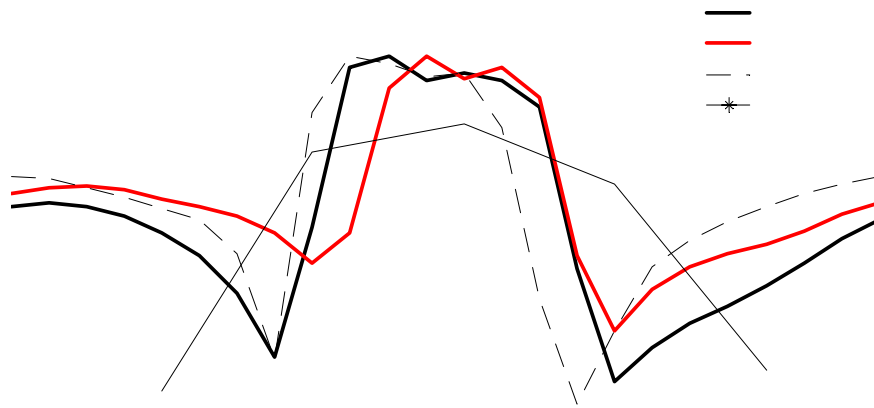
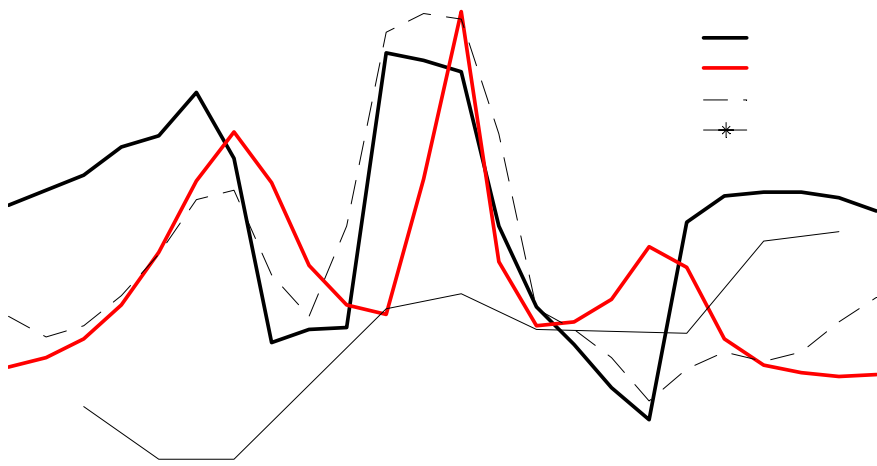


Figure 5 Azimuthal distribution at level 4 at 24, 28 and 31 s.



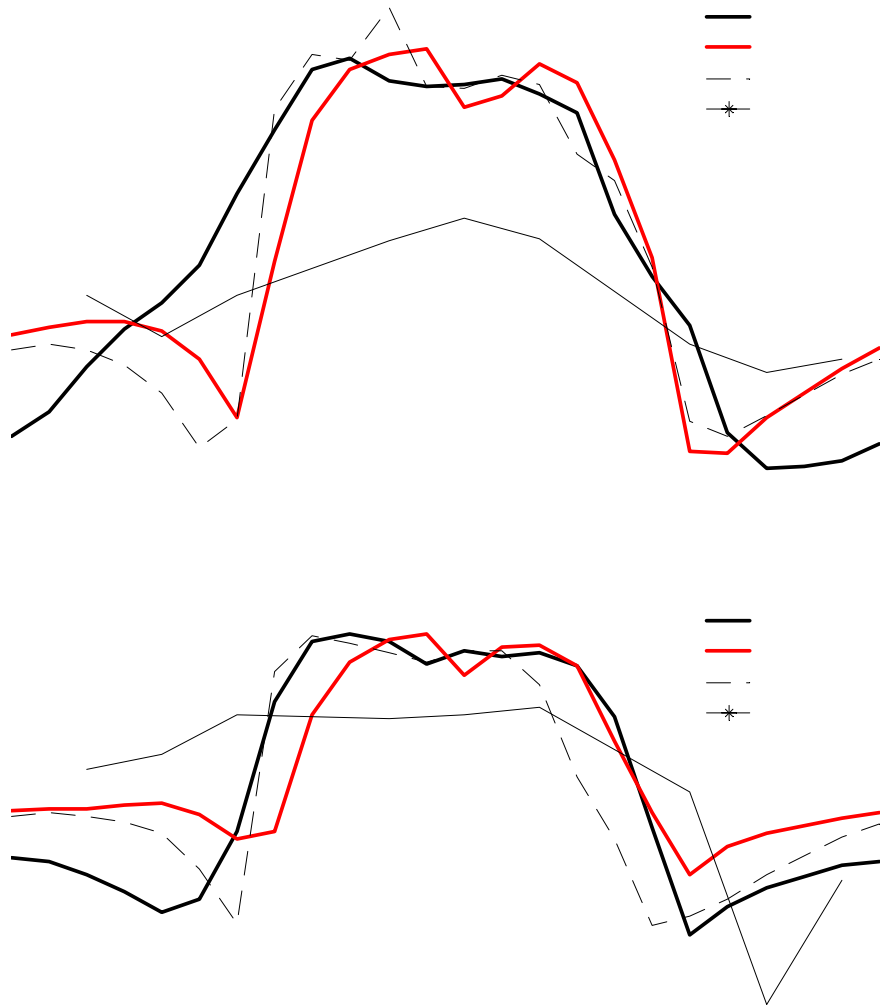
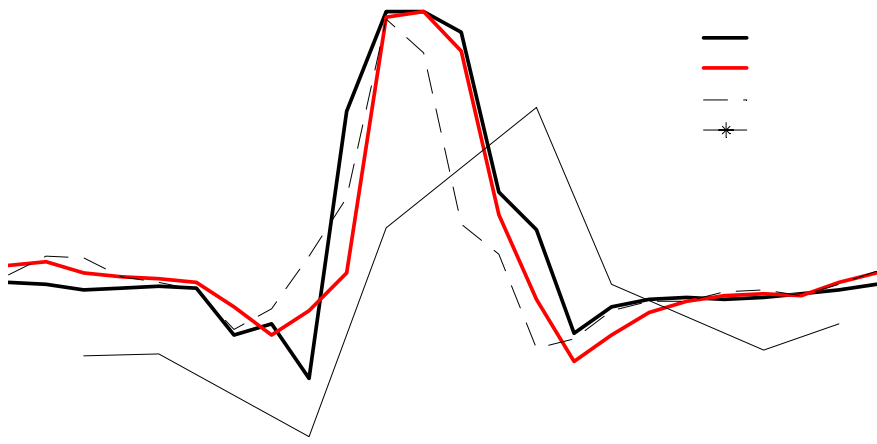


Figure 6 Azimuthal distribution at level 6 at 24, 28 and 31 s.



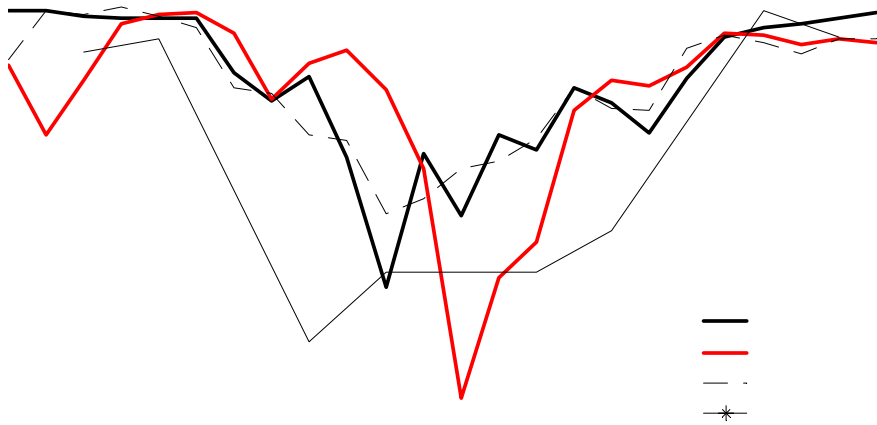
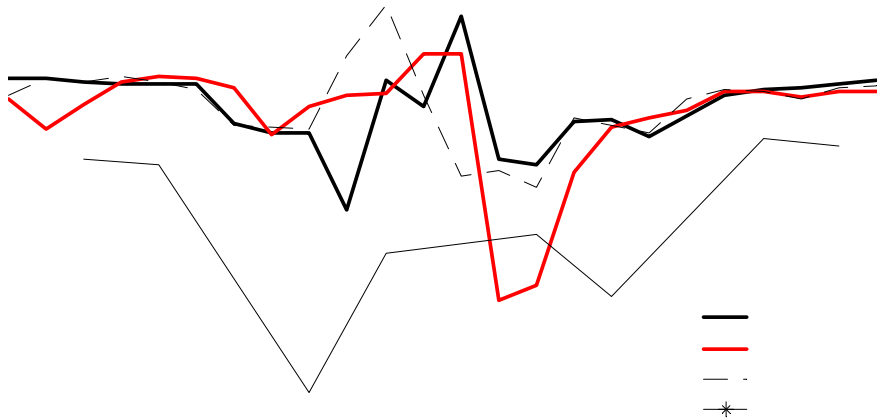


Figure 7 Azimuthal distribution at level 8 at 24, 28 and 31 s.